ISSN:2277-3754
International Journal of Engineering and Innovative Technology (IJEIT)
Volume 1, Issue 2, February 2012

Space vector PWM Technique for 3phase voltage source inverter using Artificial Neural Network

Bandana, K.Banu priya, JBV Subrahmanyam, Ch.Sikanth, M.Ayyub

Abstract*— Space vector pulse width modulation (SVPWM) is an optimum pulse width modulation technique for an inverter used in a variable frequency drive applications. It is computationally rigorous and hence limits the inverter switching frequency. A neural network has the advantage of very fast implementation of an SVPWM algorithm that can increase the inverter switching frequency. This paper proposes a neural Network based SVPWM technique for a three-phase voltage source inverter in under modulation region. The scheme has been simulated and implemented on a V/Hz controlled 5-hp, 50-Hz, and 230V induction motor drive. The simulation results are given to validate the performances of the drive with artificial neural network based SVPWM.

***Index Terms*—Space vector pulse width modulation, neural network, voltage source inverter.**

I. INTRODUCTION

Variable frequency ac drives are increasingly replacing dc drives in a number of industrial applications due to advantages in size, reliability and efficiency. One of the main components of an ac drive is power electronic converter in the form of voltage source inverter that takes dc voltage input (may be from a rectifier) and produces a sinusoidal ac waveform. This in turn is fed to the ac electric motor. The fundamental frequency of this waveform is adjusted to produce the desired speed. In modern electric drives the modulation of switching is carried out to achieve the required ac wave shape. This is met by incorporating the duration of 'ON' & 'OFF' methods [1, 2].

The techniques to get the duration of ON interval for a particular switch depend upon the control logic or PWM technique to be adopted. In a PWM scheme the output voltage and frequency can be controlled with the help of the switching inside the inverter. The switch may be MOSFET, IGBT etc with anti parallel connected diodes. Different PWM schemes such as sinusoidal PWM compares a high frequency triangular carrier with three sinusoidal reference signals, known as the modulating signals, to generate the gating signals for the inverter switches but having a disadvantage that it contains third harmonic in output[3]. To the cancellation of the third-harmonic components and better utilization of the dc supply, the third harmonic injection PWM scheme is preferred in three-phase applications. Space vector modulation technique has advantage of an optimal output and also reduces harmonic content of the output voltage/current [4]. Space vector PWM (SVPWM) has the advantages of lower harmonics and a higher modulation index in addition to the features of complete digital implementation by a single chip microprocessor, because of its flexibility of manipulation, SVPWM has increasing application in power converters and motor control.

The application of artificial neural network (ANN) is recently growing in power electronic systems. A feed forward ANN implements nonlinear input–output mapping. The computational delay of this mapping becomes negligible, if parallel architecture of the network is implemented by an application-specific integrated circuit (ASIC) chip [5]. A feed forward carrier-based PWM technique, Such as SVM, can also be looked upon as a nonlinear mapping phenomenon where the command phase voltages are sampled at the input and the corresponding pulse width patterns are established at the output. Therefore, it appears logical that a back propagation-type ANN that has high computational capability can implement an SVM algorithm. The ANN can be conveniently trained offline with the data generated by calculation of the SVM algorithm. ANN has inherent learning capability that can give improved precision by interpolation unlike the standard lookup table method [5].

The ANN-based SVPWM of a voltage-fed inverter can also use competitive neural network architecture to identify the inverter switching states and the corresponding voltage magnitudes for the impressed command voltage. This paper describes feed- forward ANN-based SVPWM that covers linear modulation region. In the beginning, the SVPWM theory has been briefly reviewed with mathematical analysis for the linear modulation range. Then equations for algorithms have been developed in detail. A back propagation type feed forward ANN is trained offline with the data generated by this simple algorithm [5].

II. SPACE VECTOR PWM – A REVIEW

This section is devoted to the development of Space vector PWM for a two-level voltage source inverter in linear region of operation [6]. As seen from Fig 1, there are six switching devices and only three of them are independent as the operation of two power switches of the same leg are complimentary. The combination of these three switching states gives out eight possible space voltage vectors. The space vectors forms a hexagon with 6 distinct sectors, each spanning 60 degrees in space. At any instant of time, the inverter can produce only one space vector. In space vector PWM a set of three vectors (two active and a zero) can be selected to synthesize the desired voltage in each switching period. All of the eight modes are shown in Table.1.

Out of eight topologies six (states 1-6) produce a non-zero output voltage and are known as active voltage vectors and

ISSN:2277-3754
International Journal of Engineering and Innovative Technology (IJEIT)
Volume 1, Issue 2, February 2012

the remaining two topologies (states 0 and 7) produce zero output voltage (when the motor is shorted through the upper or lower transistors) and are known as zero voltage vectors, various possible switching states are shown in Fig 2.

Space vector is defined as [6],

$$\underline{v}_s^* = \frac{2}{3}\left(v_a + \underline{a}v_b + \underline{a}^2 v_c\right) \qquad (1)$$

Where $\underline{a} = \exp\left(j2\pi/3\right)$.

The space vector is a simultaneous representation of all the three-phase quantities [14]. It is a complex variable and is function of time in contrast to the phasors. Phase-to-neutral voltages of a star-connected load are most easily found by defining a voltage difference between the star point *n* of the load and the negative rail of the dc bus *N*. The following correlation then holds true:

$$\begin{aligned} v_A &= v_a + v_{nN} \\ v_B &= v_b + v_{nN} \qquad (2) \\ v_C &= v_c + v_{nN} \end{aligned}$$

Since the phase voltages in a start connected load sum to zero, summation of equation (2) yields

$$v_{nN} = (1/3)(v_A + v_B + v_C) \qquad (3)$$

Substitution of (3) into (2) yields phase-to-neutral voltages of the load in the following form:

$$\begin{aligned} v_a &= (2/3)v_A - (1/3)(v_B + v_C) \\ v_b &= (2/3)v_B - (1/3)(v_A + v_C) \qquad (4) \\ v_c &= (2/3)v_C - (1/3)(v_B + v_A) \end{aligned}$$

Phase voltages are summarized and their corresponding space vectors are listed in Table 1. The eight vectors including the zero voltage vectors can be expressed geometrically as shown in fig.3. Each of the space vectors, in the diagram represent the six voltage steps developed by the inverter with the zero voltages V_0 (0 0 0) and V_7 (1 1 1) located at the origin. Space Vector PWM require to averaging of the adjacent vectors in each sector. Two adjacent vectors and zero vectors are used to synthesis the input reference determined from Fig.4 for sector I. Using the appropriate PWM signals a vector is produced that transitions smoothly between sectors and thus provide sinusoidal line to line voltages to the motor.

In order to generate the PWM signals that produces the rotating vector. The PWM time intervals for each sector is determined from Fig. 4 for sector I as

Along real axis:

$$V_1\frac{T_1}{T_s} + (V_2\cos 60)\frac{T_2}{T_s} = mV_S\cos\alpha \qquad (5)$$

Along imaginary axis:

$$0 + (V_2\sin 60)\frac{T_2}{T_s} = mV_S\sin\alpha \qquad (6)$$

Solving equations (5) and (6)

$$T_1 = T_S\frac{mV_S\sin(60-\alpha)}{V_1\sin 60}$$

$$T_1 = T_s\frac{m\frac{1}{2}V_{DC}\sin(60-\alpha)}{\frac{2}{3}V_{DC}\sin 60}$$

$$\boxed{T_1 = \frac{\sqrt{3}}{2}mT_S\sin(60-\alpha)} \qquad (7)$$

$$T_2 = T_S\frac{mV_S\sin\alpha}{V_2\sin 60}$$

$$\boxed{T_2 = \frac{\sqrt{3}}{2}mT_S\sin(\alpha)} \qquad (8)$$

$$\boxed{T_0 + T_7 = T_s - (T_1 + T_2)} \qquad (9)$$

Generalizing the time expressions gives

$$T_1 = \frac{\sqrt{3}}{2}mTs\sin\left(\frac{k\pi}{3} - \alpha\right) \qquad (10)$$

$$T_2 = \frac{\sqrt{3}}{2}mTs\sin\left(\frac{(k-1)\pi}{3} - \alpha\right);\ \text{k=1, 2, 3...} \qquad (11)$$

The time of application of active and zero space vectors for all six sectors are given in Table 2 [13]. The periods T_1, T_2 and T_0 depends only on the reference vector amplitude Vs and the angle 'α'. This shows that the period T_1, T_2 and T_0 are the same in all sectors for the same V_S and 'α' position. In the under modulation region, the vector V_S always remains within the hexagon. The mode ends in the upper limit when V_S describes the inscribed circle of the hexagon. Modulation Index *MI* ***(m)*** is given by

$$m = \frac{Vs^*}{V_{1Sixstep}}$$

Where, V_S = input reference vector magnitude

$V_{1Six\ step}$ = fundamental peak value $\frac{2V_{DC}}{\pi}$ of the six step output.

The maximum value of input reference is the radius of largest circle inscribed in the hexagon given by

$$V_s^* = \frac{2}{3}V_{DC}\cos(30^0) = 0.577V_{DC}$$

Therefore, maximum modulation index

$$\boxed{m = \frac{Vs^*}{V_{1SW}} = \frac{0.577V_{DC}}{\frac{2}{\pi}V_{DC}} = 0.907} \qquad (12)$$

This means that 90.7% of the fundamental of the six step wave is available in the linear region, compared to 78.55% in the sinusoidal PWM [7].

ISSN:2277-3754
International Journal of Engineering and Innovative Technology (IJEIT)
Volume 1, Issue 2, February 2012

III. NEURAL NETWORK BASED SPACE VECTOR PWM

The first step that involves in the implementation of neural network based space vector PWM of a voltage source inverter is generation of training data. The training data is generated by using eqs. (1), (2), (3).the angle subnet is trained with an angle interval of 2° in the range of $0-360^\circ$.

The phase-A turn ON time can be expressed as

$$T_{A=ON}=\begin{cases}\frac{t_0}{4}=\frac{T_s}{4}+K.V^*\left[-\sin\left(\frac{\pi}{3}-\alpha^*\right)-\sin(\alpha^*)\right], S=1,6\\ \frac{t_0}{2}+t_b=\frac{T_s}{4}+K.V^*\left[-\sin\left(\frac{\pi}{3}-\alpha^*\right)+\sin(\alpha^*)\right], S=2\\ \frac{t_0}{2}+t_0+t_b=\frac{T_s}{4}+K.V^*\left[\sin\left(\frac{\pi}{3}-\alpha^*\right)+\sin(\alpha^*)\right], S=3,4\\ \frac{t_0}{2}+t_a=\frac{T_s}{4}+K.V^*\left[\sin\left(\frac{\pi}{3}-\alpha^*\right)-\sin(\alpha^*)\right], S=5\end{cases}$$

Equation (4) can be written in the general form

$$T_{A-ON}=T_s/4+f(V^*)g_A(\alpha^*)$$

Where $f(V^*)$ is the voltage amplitude scale factor and

$$g_A(\alpha^*)=\begin{cases}K\left[-\sin\left(\frac{\pi}{3}-\alpha^*\right)-\sin(\alpha^*)\right], S=1,6\\ K\left[-\sin\left(\frac{\pi}{3}-\alpha^*\right)+\sin(\alpha^*)\right], S=2\\ K\left[\sin\left(\frac{\pi}{3}-\alpha^*\right)+\sin(\alpha^*)\right], S=3,4\\ K\left[\sin\left(\frac{\pi}{3}-\alpha^*\right)-\sin(\alpha^*)\right], S=5\end{cases}$$

Fig.(3) shows schematic of the ANN based SVPWM inverter. The input signal to the neural network is angle θ. Fig.(4) shows the neural network model. The model uses a multilayer function in the first and second layer respectively. The Neural network uses one neuron at the input 25 neurons in the hidden layer and three output neurons. The digital words corresponding to turn on time are generated by multiplying the output of neural network with V^*T_S and then adding $T_s/4$ as shown in figure. The PWM signals are then generated by comparing turn-On time with a triangular reference having time period of T_S and amplitude $T_s/2$ .the PWM signals are then applied to the inverter. The back propagation algorithm in the Matlab toolbox is used for the training. The angle subnet takes 101650 epochs for training with an error 0.53%.The value of size and the corresponding training time are, thus reasonably small.

IV. DRIVE SYSTEM PARAMETERS

DC-link voltage 300 V
Sampling time (T_s) 200 μs
Induction motor 5 hp 230 V four pole, squirrel cage
Frequency range: 0-50 Hz
Stator resistance (R_s): $0.5814\,\Omega$
Rotor resistance (R_r): $0.4165\,\Omega$
Stator leakage inductance (L_{ls}): 3.479 mH
Rotor leakage inductance (L_{lr}): 4.15 mH
Mutual inductance (L_m): 78.25mH
Rotor inertia (J): 0.1 kg.m^2

V. SIMULINK MODEL AND RESULTS

The Simulink model used to simulate model results on computer is shown in fig. (7).Fig. (8) Shows the characteristics of speed of induction motor. In the starting speed of motor increases very sharply and reaches to 1700 rpm after 0.1 seconds. Some oscillations are followed till the motor catches the reference speed (i.e. 1500 rpm) in 0.3 seconds. At 0.75 seconds when load torque is changed from 0 Nm to 10 Nm it attains a value slightly lower than the reference speed as shown in the figure. This lower value of speed is due to increase in torque and the system is operating in open loop. Fig.(9) shows torque characteristics for load torque (Tl) and developed torque (Te). In the starting the applied torque is zero and developed torque is very high for few seconds (till 0.125 second). After some fluctuation it attains a value of zero in 0.25 seconds, as Tl=0. When load torque is increased to a value 10 Nm at 0.75 seconds. The developed torque also attains the value of 10 Nm following some transients as depicted in figure. The stator and rotor current for dynamic conditions are shown in fig.(10) &(11) respectively. The current shows the expected trend and are sinusoidal in nature. These currents have high initial values during starting due to starting transients, as the induced emf takes time to develop its rated value. After these transients are over, the current settles at its steady state values after 0.2 sec. The currents (stator and rotor) get higher values when load torque of 10 Nm is applied at 0.75 sec. These can be seen in the figure.

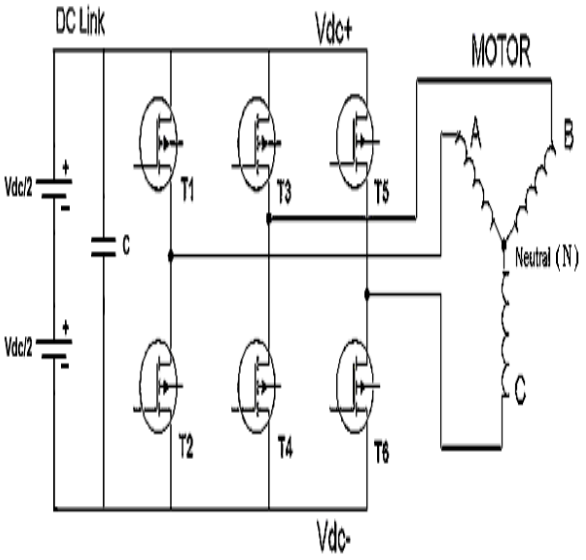

Fig. 1. Power circuit of a three-phase voltage source inverter [12]

ISSN:2277-3754
International Journal of Engineering and Innovative Technology (IJEIT)
Volume 1, Issue 2, February 2012

Table-1 possible modes of operation of a three-phaseVSI[12]

State	On Devices	Van	Vbn	Vcn	Space Voltage Vector
0	T2, T4, T6	0	0	0	$V_0(000)$
1	T1, T4, T6	2Vdc/3	-Vdc/3	-Vdc/3	$V_1(100)$
2	T1, T3, T6	Vdc/3	Vdc/3	-2Vdc/3	$V_2(110)$
3	T3, T2, T6	-Vdc/3	2Vdc/3	-Vdc/3	$V_3(010)$
4	T2, T3, T5	-2Vdc/3	Vdc/3	Vdc/3	$V_4(011)$
5	T2, T4, T5	-Vdc/3	-Vdc/3	2Vdc/3	$V_5(001)$
6	T1, T4, T5	Vdc/3	-2Vdc/3	Vdc/3	$V_6(101)$
7	T1, T3, T5	0	0	0	$V_7(111)$

Table 2 – Application of time [13]

Sector I $(0 \le \omega t \le \frac{\pi}{3})$	Sector II $(\frac{\pi}{3} \le \omega t \le \frac{2\pi}{3})$	Sector III $(\frac{2\pi}{3} \le \omega t \le \pi)$
$T_1 = \frac{\sqrt{3}}{2} m T_s \cos(\omega t + \frac{\pi}{6})$	$T_2 = \frac{\sqrt{3}}{2} m T_s \cos(\omega t + \frac{11\pi}{6})$	$T_3 = \frac{\sqrt{3}}{2} m T_s \cos(\omega t + \frac{3\pi}{2})$
$T_2 = \frac{\sqrt{3}}{2} m T_s \cos(\omega t + \frac{3\pi}{2})$	$T_3 = \frac{\sqrt{3}}{2} m T_s \cos(\omega t + \frac{7\pi}{6})$	$T_4 = \frac{\sqrt{3}}{2} m T_s \cos(\omega t + \frac{5\pi}{6})$
$T_0 + T_7 = T_s - T_1 - T_2$	$T_0 + T_7 = T_s - T_2 - T_3$	$T_0 + T_7 = T_s - T_3 - T_4$
Sector IV $(\pi \le \omega t \le \frac{4\pi}{3})$	**Sector V** $(\frac{4\pi}{3} \le \omega t \le \frac{5\pi}{3})$	**Sector VI** $(\frac{5\pi}{3} \le \omega t \le 2\pi)$
$T_4 = \frac{\sqrt{3}}{2} m T_s \cos(\omega t + \frac{7\pi}{6})$	$T_5 = \frac{\sqrt{3}}{2} m T_s \cos(\omega t + \frac{5\pi}{6})$	$T_6 = \frac{\sqrt{3}}{2} m T_s \cos(\omega t + \frac{\pi}{2})$
$T_5 = \frac{\sqrt{3}}{2} m T_s \cos(\omega t + \frac{\pi}{2})$	$T_6 = \frac{\sqrt{3}}{2} m T_s \cos(\omega t + \frac{\pi}{6})$	$T_1 = \frac{\sqrt{3}}{2} m T_s \cos(\omega t + \frac{11\pi}{6})$
$T_0 + T_7 = T_s - T_4 - T_5$	$T_0 + T_7 = T_s - T_5 - T_6$	$T_0 + T_7 = T_s - T_1 - T_6$

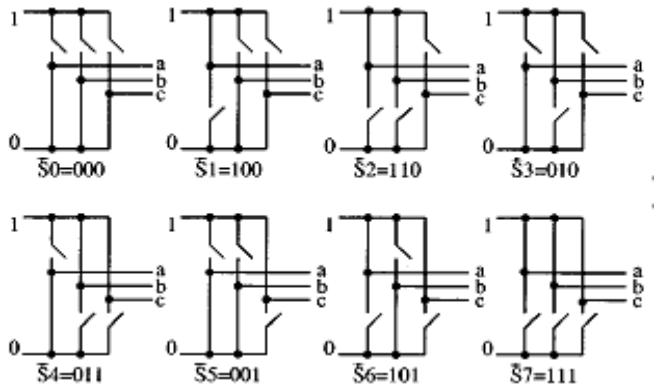

Fig. 2 -The switches position during eight topologies [12]

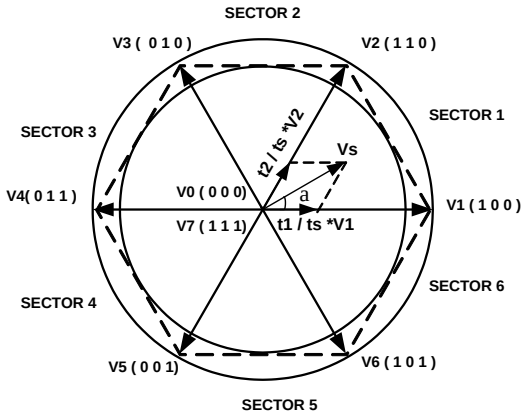

Fig. 3 - Space Vector representation of Line to Neutral Voltages [13]

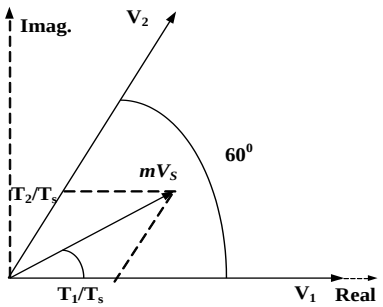

Fig. 4- Principle of time calculation for SVPWM in sector I[13]

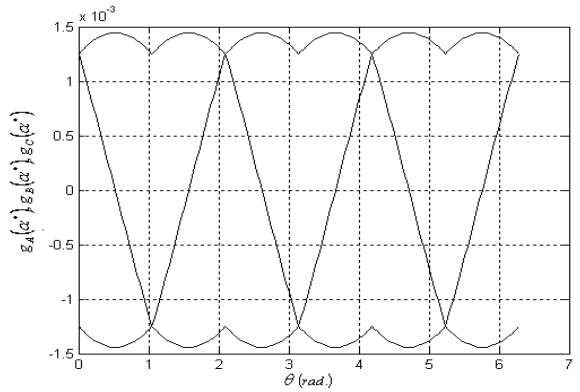

Fig.5 Turn –on pulse width function of phase A, B, C as a function of Angle θ in different sectors [13]

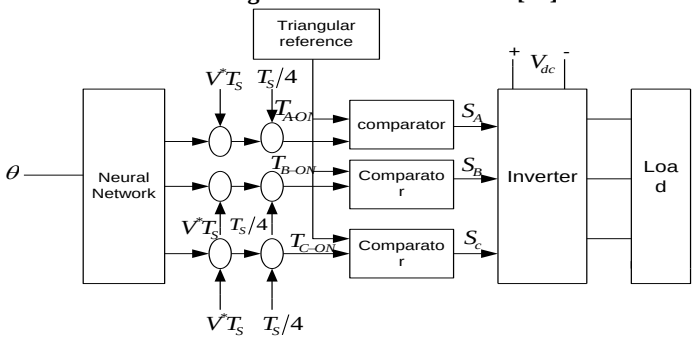

Fig.6 Schematic of the ANN based SVPWM inverter [5]

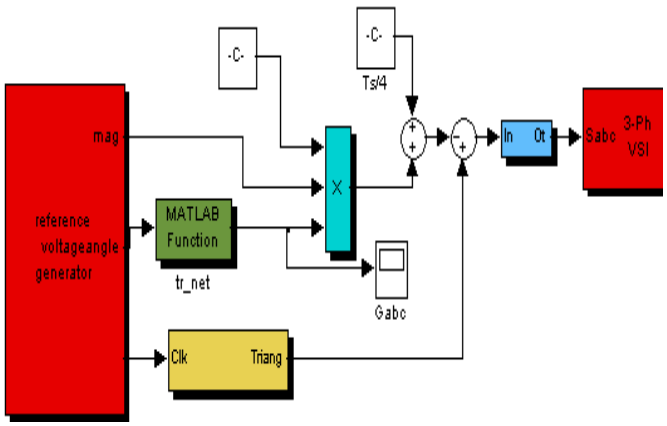

Fig.7 Model of Ann based space vector PWM controller for voltage Fed inverter Induction motor drive

ISSN:2277-3754
International Journal of Engineering and Innovative Technology (IJEIT)
Volume 1, Issue 2, February 2012

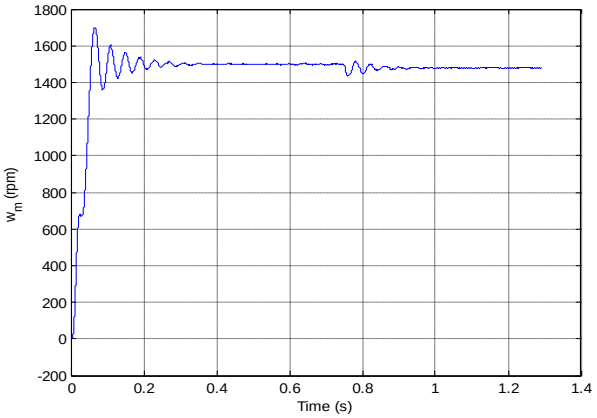

Fig.8 Speed characteristics

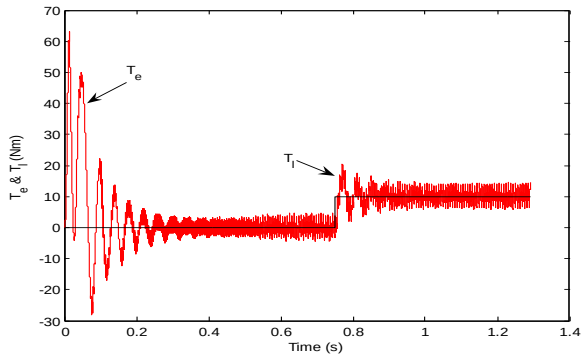

Fig.9 Torque characteristics

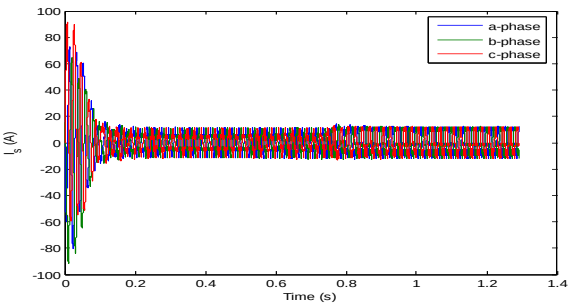

Fig.10 Stator current waveform

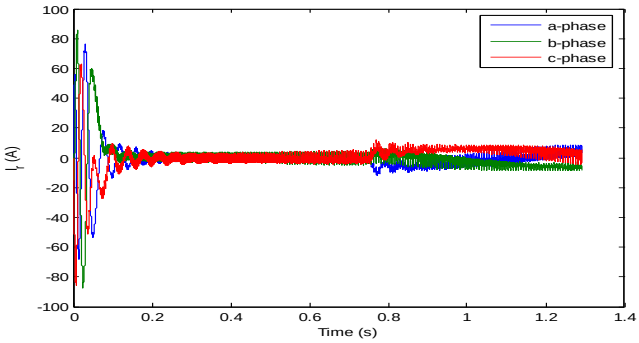

Fig.11 Rotor current waveform

VI. CONCLUSION

A neural-network-based space-vector modulator has been described that operates very well in under modulation region. The digital words corresponding to turn-on time are generated by the ANN and then converted to pulse widths through a single timer. The scheme uses a back propagation-type feed forward network. The training data and training time are reasonably small. The method can operate from dc (zero frequency). The scheme has been fully implemented and evaluated with a V/Hz-controlled induction motor drive, and gives excellent performance. The PWM controller is currently being used in a stator-flux-oriented vector-controlled induction motor drive. The ANN-based SVM can give higher switching frequency, which is not possible by conventional DSP-based SVM. The switching frequency can be easily extended up to 50 kHz if the ANN is implemented by a dedicated hardware ASIC chip.

VII. FUTURE ENHANCEMENT OF WORK

The ANN-based SVM can give higher switching frequency, which is not possible by conventional DSP-based SVM. The switching frequency can be easily extended up to 50 kHz if the ANN is implemented by a dedicated hardware ASIC chip.

REFERENCES

[1] W. vander Broek, H. C. Skudelny, and G. V. Stanke, “Analysis and realization of PWM based on voltage space vectors”, IEEE Trans. Ind. Applicat., vol. 24, no. 1, pp. 142–150, 1988.

[2] Grahame Holmes and Thomas A. Lipo , “ Pulse Width Modulation For Power Converters – Principles and Practices”, IEE Press, Wiley Publications2000.

[3] Blasko, “A hybrid PWM strategy combining modified space vector and triangle comparison methods”, in IEEE PESC Conf. Rec., 1996, pp.1872–1878.

[4] S. Patel and R. G. Hoft, “Generalized techniques of harmonic elimination and voltage control in thyristor inverters: Part I—Harmonic elimination,” IEEE Trans. Ind. Applicat., vol. 9, pp. 310–317, May/June 1973.

[5] J.O.P. Pinto, B.K. Bose, L.E. Borges da Silva and M.P. Kazmierkowski, “A Neural Network based space vector pwm controller for voltage fed inverter induction motor drive”, IEEE Trans, Ind. Appl. Vol. 36, No.6, pp.1628-1636 November/December 2000.

[6] J. Kerkman, B. J. Seibel, D. M. Brod, T. M. Rowan, and D. Leggate, “A simplified inverter model for on-line control and simulation”, IEEE Trans. Ind. Applicat., vol. 27, no. 3, pp. 567–573, 1991.

[7] Simon Haykin, “Neural Networks”, ND prentice Hall, 2004.

[8] Muthuramalingam and S.Himavathi.” Performance Evaluation of a Neural Network based General Purpose Space Vector Modulator”, IJECSE Vol.1, No.1, pp.19-26, April 2007.

[9] K. Zhou and D. Wang, “Relationship between space vector modulation and three phase carrier base PWM – A comprehensive analysis”, IEEE Trans, Ind. Electr, Vol 49, No.1,pp 186-196, Feb. 2002.

[10] akhshai, J. Espinoza, G. Joos, and H. Jin, “A combined artificial neural network and DSP approach to the implementation of space vector modulation techniques, “In Conf, Rec. IEEE-IAS Annu, Meeting,. 1996 pp.934-940.

[11] H.W. Van Der Brock, H.C. Skundelny and G.V. Stanke, “Analysis and realization of a pulse width modulator based on

voltage space vectors', IEEE Trans Ind. Appl., 24. pp. 140-150, Jan/Feb 1998.

[12] O.Ogasawara, H. Akagi, and Nabel, " A novel PWM scheme of voltage source inverters based on space vector theory," in proc. EPE European conf. Power Electronics and Applications pp. 1197-1202, 1989.

[13] S.R. Bowes and Y.S. Lai, "The relationship between space vector modulation and regular-sampled PWM, "IEE Trans. Power Electron, Vol. 14, pp. 670-679, Sept. 1997.

[14] Reichmann's, Bernet.S, "A Comparison of Three-Level Converters versus Two-Level Converters for Low-Voltage Drives, Traction, and Utility Applications,"IEEE Transaction on Industry Applications, Vol.41, No. 3, pp: 855-865, May/June, 2005.